

Underground rock engineering to match the rock's behaviour - Challenges of managing highly stressed ground in civil and mining projects – (Executive Summary)

Kaiser, P.K.

Laurentian University, Sudbury, Ontario, Canada

Copyright 2016 ARMA, American Rock Mechanics Association

This paper was prepared for presentation at the 50th US Rock Mechanics / Geomechanics Symposium held in Houston, Texas, USA, 26-29 June 2016.

ABSTRACT:

The key messages of the MTS lecture are outlined here in the form of a brief executive summary with selected extracts from the slide deck. The reader is referred to related publications for detailed explanations.

In the spirit of the conference theme “new exciting advances in rock mechanics”, this lecture introduces several recent advances that are awaiting application in engineering practice and aims at opening new paths of discovery by questioning implicit assumptions in standard engineering approaches.

1 PREAMBLE

“No challenge is too big for rock specialists with the right know-how and skill.”



Figure 1 Rock climbers or rock specialists at work on El Capitan in Yosemite National Park (CA) (insert courtesy: G. van Aswegen)

1.1 Safety share

By reference to Figure 1, the same applies to safety, “if you put your mind to safety, you get safety and good performance, too.”

2 THE STORYLINE

A robust rock engineering solution in underground mining or construction must respect the complexity and variability of the geology, consider the practicality and efficiency of construction and provide safe and effective rock support.

For this purpose it is essential to anticipate the rock mass and excavation behaviour early in the design process, i.e., at the tender stage before excavation techniques are chosen and designs are locked in through construction contracts.

Whereas it is possible in most engineering disciplines to select the most appropriate material for a given engineering solution. In rock engineering, a design must be made to fit the rock; not vice versa.

Lessons learned from excavation failures (Figure 2) tell us that stressed rock at depth is less forgiving and that advances in rock mechanics demand a full comprehension of the behaviour of stress-damaged rock near excavations.



Figure 2 Examples of excavation instabilities in stressed rock.

Comprehension in this context means explaining all observations such that fiction can be separated from reality and our engineering models and methods become congruent with the actual behaviour of a rock mass. This summary of the lecture presents a discussion of aspects of underground rock engineering where dichotomies exist and gaps between reality and current practices have to be closed by the application of recent advances in rock mechanics to arrive at sound rock engineering solutions.

3 EXCAVATION BEHAVIOUR

It is well-known that the excavation behaviour depends on the rock mass quality or strength (horizontal axis in Figure 3) and the mining-induced stress (vertical axis on the right; [9]). What is often ignored in practice, particularly when using empirical methods, is that mining-induced stress changes or variations in stress paths may drastically alter the excavation failure mode. During the life span of an excavation, the behaviour mode may therefore change and with it the applicable engineering models may have to be changed accordingly.

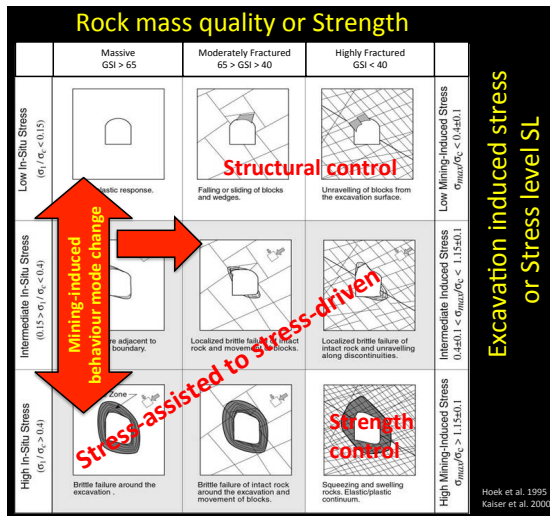


Figure 3 Excavation behaviour matrix with indication of anticipated failure mode changes resulting from mining-induced stress-paths (after [3] and [8]).

As was illustrated by reference to field measurements from a caving operation, the stress level index $SL = (3\sigma_1 - \sigma_3) / UCS$ may change rapidly over the life span of an excavation from an initially rather favourable condition with $k = \sigma_1/\sigma_3$ ranging from 0.5 to 2 to very unfavourable conditions

for k exceeding 3 with high stress concentrations (tangential stresses exceeding $8\sigma_1$) and simultaneous relaxation (σ_3 less than zero).

At greater depths, the behaviour of underground excavations is therefore often affected or dominated by stress-fracturing (gray boxes in Figure 3) and may change drastically over its life span as stress changes will alter instability mechanisms. Because rock mass models typically only reflect one behaviour mode they become frequently deficient when changes occur. A robust engineering design has to respect these behavioural changes.

4 DESIGN BASED ON FICTION OR MATCHING REALITY ?

Whereas it is always necessary to make some simplifications for most engineering designs, as paraphrased by R. Sessions after A. Einstein, they should be as simple as possible but not simpler – or, in engineering terms “a little fiction is ok but not too much”.

By exploring dichotomies between fiction and reality in engineering approaches, including numerical modelling and empirical methods, deficiencies in designs can be identified and eventually overcome, and advances in rock engineering can be implemented and new advances can be made. There is a need to close such gaps by matching designs to the actual rock mass and excavation behaviour. Dichotomies between fiction and reality are explored for brittle failing rock with respect to:

- Failure criteria (peak and residual);
- Depth failure around excavations;
- Volumetric behaviour of broken rock;
- Characterization for rock mass strength determination; and
- Rock mass heterogeneity.

For details related to rock mass characterization and for implications with respect to support design, the reader is referred to the on-line ISRM lecture [4] and the Sir Muir Wood lecture [5].

4.1 Failure criteria for brittle rock

Tensile stresses induced during loading in heterogeneous rock lead to Griffith-type extension fracturing with the consequence of depressing the failure envelope (Figure 4) in the low confinement

zone (at approximately $\sigma_3 < UCS/10$) where fracture propagation causing spalling cannot be suppressed by the available confining pressure. The resulting failure envelope for rock affected by stress-fracturing is s-shaped or tri-linear; not linear (Mohr-Coulomb) or continuously curved (Hoek-Brown) ([7]).

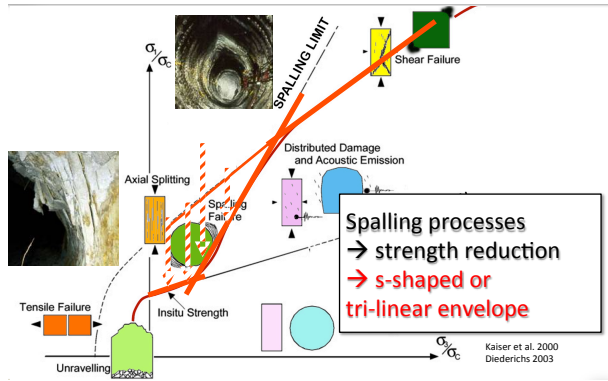


Figure 4 Principal stress space showing depressed failure envelope in low confinement range and related excavation failure processes: spalling, notching, and shear rupture.

4.1.1 The Mohr-Coulomb error

Schofield [11], by reference to Taylor’s work and to Terzaghi’s use of the Mohr-Coulomb (MC) criteria, pointed out that it is a serious error to assume that the cohesive and frictional strength components are simultaneously mobilized. Supported by [9], it is now well-understood that the mobilization of the cohesive and frictional components of rock and rock mass strength is strain-dependent as reflected in the following revised version of the MC strength equation with cohesion, effective stress internal to the rock and the dilation angle depending on the plastic strain:

$$\tau = c(\epsilon) + \sigma'(\epsilon) \tan(\varphi + i(\epsilon))$$

Rock mass failure forecasting thus becomes highly sensitive to the assumed stress-strain characteristics, rendering many frequently adopted models (e.g., elastic, perfectly brittle plastic models) as fiction, i.e., far from reality.

4.1.2 Post-peak strength (PPS)

It is frequently assumed that the post-peak strength (PPS) is defined by the residual strength. This assumption becomes fiction and is not congruent with reality when the actual induced plastic strain is less than the strain needed to reach the

residual strength. This is the case in most engineering problems, particularly for civil engineering applications. By considering Marble (Figure 5) as an analogue for a rock mass, it can be seen that the PPS is strain-dependent, leading to a bi-linear PPS envelope with a cohesion intercept and a change in slope at the brittle ductile transition (σ_3^*). With increasing strain, the mobilized PPS (mPPS) decreases and eventually reaches the residual PPS. The cohesion intercept and the location of the transition point of the mPPS are strain-dependent and the residual strength is, for most rocks, only reached at large strains (strains larger than typically encountered in underground structures).

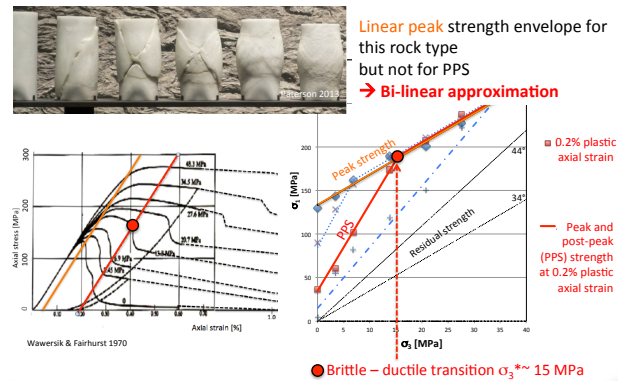


Figure 5 Marble as rock mass analogue indicating strain-dependent bi-linear post-peak strength (PPS) envelopes with brittle-ductile transition at σ_3^* (modified after [12]). The peak strength and three mobilized PPS envelopes are shown in blue and red.

Rock mass failure simulations utilizing purely frictional post-peak strength envelopes, with the PPS set equal to the residual strength, tend to underestimate the mobilized PPS and consequently lead to excessively large depth of yield predictions.

4.1.3 Strength degradation

When adopting GSI-based rock mass strength equations [3], it is implicitly assumed that the degree of interlock is sufficiently small such that rock block formed by open joints can rotate during the failure process. In massive to moderately jointed rock this is not the case and the strength is controlled by stress-fracturing of rock blocks, rock bridges and asperities, and by the dilation of highly interlocked rock fragments. Hence, the strength degradation from the intact rock strength

is much less at elevated confining pressures than conventionally assumed, at least at strains typically imposed in practice. Consequently, the rock mass is much stronger than anticipated by the standard models (see [1]).

4.1.4 Failure envelopes for brittle rock

If the s-shaped peak strength envelope introduced in Figure 4 is fitted as an approximation by Hoek-Brown or Mohr-Coulomb parameters, unconventionally high m_b - and a -values emerge (see [4] and Figure 6).

Furthermore, the post-peak strength (see Figure 5) should rarely be set equal to the residual strength because of high initial post-peak rock mass dilation (see [4] and Figure 6).

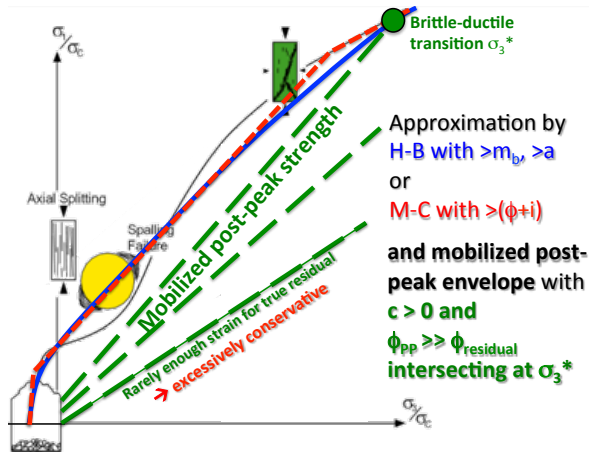


Figure 6 Illustration of means for approximation of s-shaped failure criterion and mobilized post-peak strength envelope.

It is recommended that the PPS envelop has to honour four points on the s-shaped envelop of the rock mass: the tensile strength, the unconfined compressive strength, the mid-point of the spalling limit, and the brittle-ductile transition point at σ_3^* .

4.1.5 Inner versus outer shell behaviour

From a practical perspective, the consequence of the above findings on the rock mass behaviour and engineering design are a need to differentiate between engineering problems dominated by stress-fracturing (in the inner shell) and by shear rupture (in the outer shell). The threshold between the inner and outer shell is typically at about $\sigma_3 = UCS/10$ as shown in Figure 7.

Inner shell engineering problems are those dominated by the behaviour of the rock mass in the immediate zone surrounding an excavation where the confinement is low, i.e., in the zone where stress-fracturing can occur and block/fragment rotation is possible. Engineering challenges of support design, strainbursting, etc. fall into the class of inner shell problems.

On the other hand, engineering problems related to pillar instability fall in the outer shell class where shear rupture dominates due to sufficiently high confinement.

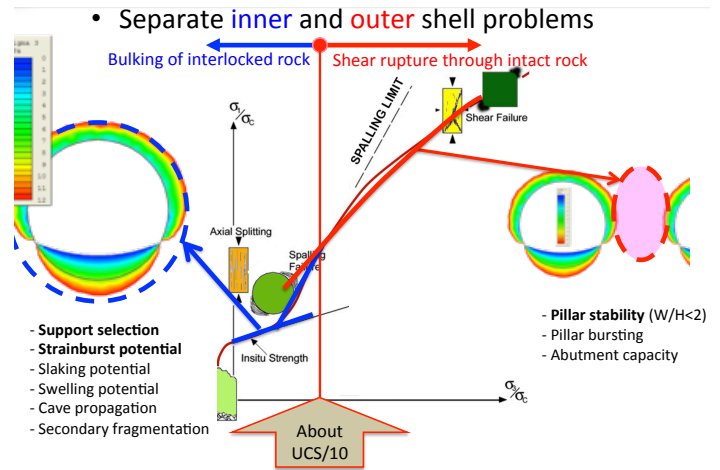


Figure 7 Zoning of stress space for inner and outer shell behaviour in underground rock engineering applications.

4.2 Depth of yield versus depth failure

Continuum models typically show indicators of yield and thus can be used to establish the depth of yield around an excavation (x in Figure 8; also shown are confinement contours for 0 to 10 MPa).

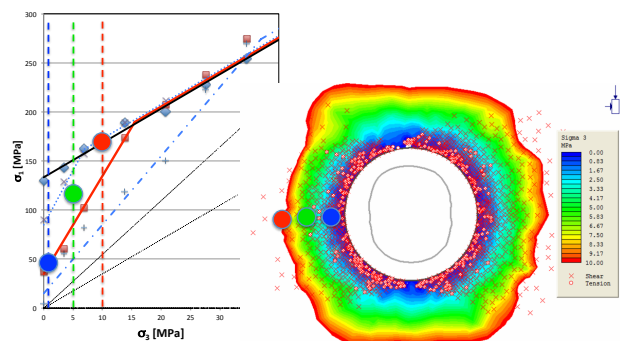


Figure 8 Right: Continuum model of tunnel showing yield locations (x and o) for $k_0 = 0.5$ and confinement contours; Left: illustration of three states at locations indicated by circles in principal stress space for marble (Figure 5).

The three coloured points in Figure 8, indicate that the rock at these locations has a substantial cohesive strength and thus, while yielded, will not fall apart and fail under gravity loading alone (will not unravel). The depth of yield is therefore not the same as the depth of failure defined as the depth to which a rock mass fails and unravels if unsupported.

The extreme normalized depth of failure d_f/a , defined as the maximum depth of notch formation or rock mass unravelling recorded in a tunnel domain with otherwise equal properties, increases linearly as a function of stress level index (up to $SL = 1$ or $\sigma_{max} = UCS$ as shown in Figure 9 in blue).

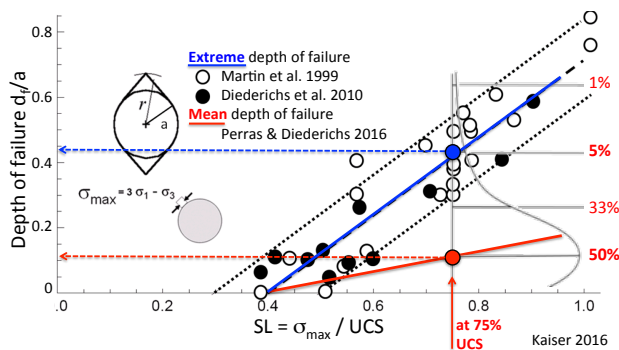


Figure 9 Depth of failure chart for extreme and mean conditions; also shown is an approximate frequency distribution at $SL = 0.75$; a = tunnel radius.

Recent work by Perras and Diederichs [10] indicate that the mean depth of failure is much smaller as indicated in red in Figure 9. Based on an assumed normal distribution shown for $SL = 0.75$, 50% of this tunnel will experience no failure or a depth of failure of less than $0.1a$. Only 5% of the tunnel in the same domain will experience an extreme depth of failure of $0.45a$ or larger. Unless local conditions deviate from the norm (e.g., due to stress variability as will be discussed below), it is highly unlikely that the depth of failure exceeds $0.65a$.

Based on the empirical data presented in Figure 9 it is today possible to not only anticipate the mean and extreme depth of failure in brittle failing rock but also to estimate the percentage of a tunnel that will experience such failure characteristics.

4.3 Dilation versus geometric bulking

Stress-fractured rock bulks due to a geometric non-fit of rock fragments when deformed past peak and loosing strength. This leads to unidirectional bulking deformations that are controlled by the excavation geometry and the imposed tangential deformation. This bulking process is not fully captured by dilation models relating strength to the volumetric strain (Figure 10). Contrary to common constitutive laws, broken rock does not gain strength despite its high dilation characteristics.

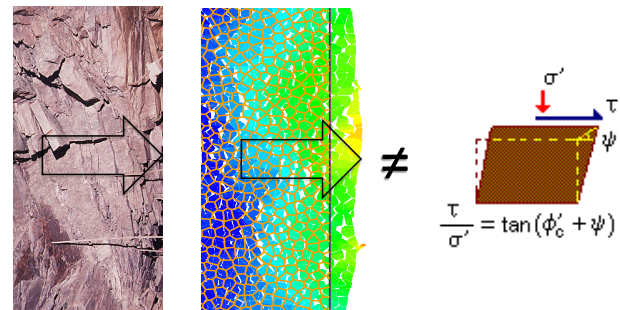


Figure 10 Unidirectional rock mass bulking due to stress-fracturing (left) reflected in Voronoi model (cartoon-like model in centre) and non-representative dilation model (right).

The geometric bulking deformation can be estimated following the semi-empirical approach outlined in [5].

4.4 Rock mass characterization

Conventional rating systems such as RMR, Q and GSI were developed and calibrated for conditions that were not dominated by large mining-induced stress changes and stress-fracturing of rock blocks bound by open joints. Hence, they are often, for example in defected rock and large strain environments, not applicable, particularly when the rock mass is massive to moderately jointed. For example, if the GSI is indiscriminately applied to conditions other than those used to develop the GSI approach, the resulting rock mass strength tends to be underestimated. This is applicable to all rating systems and is addressed in the author's ISRM on-line lecture on "Challenges of rock mass strength determination" [4].

4.5 Homogeneity versus heterogeneity

Despite today's computational capabilities many engineers (and researchers) still resort to homogeneous stress models and, if not, only consider strength heterogeneities. The impact of modulus and strength heterogeneity on the in-situ and mining-induced stresses is rarely considered. Furthermore, over-simplistic statements are frequently found in GBR's or in tender documents often suggesting that "the stress field can be approximated by the overburden weight and a stress ratio k near unity or possibly ranging from <1 to 2 ". Such simplistic conditions are rarely valid, particularly along tunnels crossing various geological domains. They often represent non-conservative baseline assumptions.

The influence of rock mass heterogeneity on the in situ stress variability in a tectonically strained setting (e.g., the Canadian Shield) is presented in [2]. The corresponding mining-induced minimum and maximum tangential stress profile for tunnels at various depths or for a tunnel progressing from surface to depth of 1600 m are presented in Figure 11.

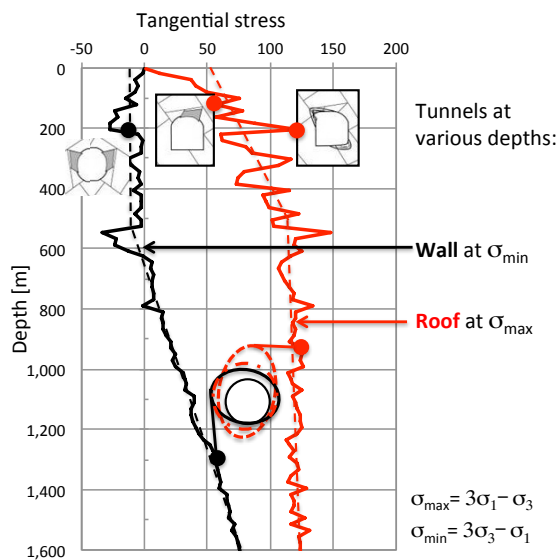


Figure 11 Example of mining-induced minimum and maximum tangential stress profiles for a circular tunnel in a tectonically strained environment. Also shown are various failure modes reflected by the behaviour matrix of Figure 3.

For a tunnel progressing in a given rock mass domain to greater depth, the minimum stress indicates stress relaxation ($\sigma_{\min} \leq 0$) to a depth of

about 600 m whereas the maximum stress is highly variable. At greater depth, the maximum tangential stress is more or less constant and the minimum stress gradually increases. The variability in stress decreases with depth for the underlying heterogeneous rockmass model that only varies in modulus at depth.

As a consequence of the stress variability, highly variable failure mechanisms are to be expected as shown by the inserts. Structurally controlled failures and overbreak together with potential stress-fracturing are to be expected at shallow depth (<600 m). At greater depth, the potential for roof and floor fracturing remains more or less constant whereas the tendency for wall fracturing gradually increasing as indicated by the changing overbreak profiles in the insert. In other words, the actual tunnel behaviour cannot be anticipated without due consideration of the anticipated stress variability. The impact of strength variability is also discussed in [2].

Two case histories in support of the high impact of stress heterogeneity can be found in [5].

5 DEFORMATION-BASED SUPPORT SELECTION

In stress-fractured ground, two mechanisms affect the excavation performance during construction: (1) raveling of broken rock resulting in short stand-up times and construction difficulties with open TBMs, and (b) large deformations caused by geometric bulking imposing large radial deformations on the support system.

The challenge of managing this highly stressed brittle rock in civil and mining projects can best be managed by the application of deformation compatible support systems. The reader is referred to the detailed analysis presented in the written version of the Sir Allan Muir Wood lecture entitled "Ground Support for Constructability of Deep Underground Excavations" [5].

It is recommended that support systems be selected based on allowable displacement criteria (i.e., Factor of Safety in terms of deformation capacity and demand, or the probability of displacements exceeding a supports displacement capacity).

The underlying principles of a deformation-based support design lead to two fundamental but practical support design axioms:

1. Control the driver of or the cause for bulking, i.e., minimize the tangential straining of the rock in the immediate vicinity of the excavation; and
2. Control the geometric bulking of stress fractured ground by rock reinforcement and the application of confining pressure.

For detailed explanations, the reader is referred to [5] and [6].

6 CONCLUSION

The various examples presented during this lecture illustrated the wide gaps between assumed and observed rock mass behaviour. Much progress has been made in recent years and these findings are available now for better and more robust engineering designs, i.e., designs that match the rock mass and excavation behaviour and thus can be constructed without undue delays and costs.

Furthermore, observations of rock behaviour to verify the applicability of design approaches are essential for sound and robust engineering. With systematic observations and correct interpretations, fiction can be replaced by models of reality and solutions can be found that fit the rock.



Figure 12 Fit solution to the rock (Illustration from brettellis.net).

The icons in the closing slide (Figure 12) indicate that “if we try to fit a solution or design to the rock as a square peg into a round hole, we cannot succeed”! Whereas one perspectives, based on observations in 100 A.D., suggested that the earth is the center of our planetary system, and another, based on calculations by Copernicus in 1540, suggests that the sun is the center, there is only one

reality. “What we thought was right yesterday may be flawed today”.

7 REFERENCES

[1] *ARMA 16-890* Bahrani N, PK Kaiser 2016. Strength degradation approach (SDA) for estimation of confined strength of micro-defected Rocks.

[2] *ARMA 16-571* Kaiser PK, S Maloney and S Yong 2016. Role of large scale heterogeneities on in-situ stress and induced stress fields.

[3] Hoek E, PK Kaiser, WF Bawden 1995. Rock Support for Underground Excavations in Hard Rock. A.A. Balkema, Rotterdam, 215 p.

[4] ISRM 2016 On-line lecture by P.K. Kaiser: Challenges in Rock Mass Strength Determination for Design of Deep Underground Excavations.

<https://www.miningexcellence.ca/?p=4194>

[5] Kaiser PK, 2016. Ground Support for Constructability of Deep Underground Excavations - Challenge of managing highly stressed brittle rock in civil and mining projects. ITA Sir Muir Wood lecture:

<https://www.ita-aites.org/en/publications/muir-wood-lecture/download/>

[6] Kaiser PK, 2014. Deformation-based support selection for tunnels in strain-burstprone ground. Deep-Mining’14, ACG (eds. Hudyma and Potvin), 227-240.

[7] Kaiser PK, B-H Kim 2008. Rock mechanics advances of underground construction and mining. Korea Rock Mech. Symp., Seoul, 1-16.

[8] Kaiser PK, MS Diederichs, CD Martin, J Sharp, W Steiner 2000. Underground works in hard rock tunneling and mining. *GeoEng 2000*, Melbourne, Australia, Technomic Publishing Co., 1: 841-926.

[9] Martin CD 1997. The effect of cohesion loss and stress path on brittle rock strength. *Canadian Geotechnical Journal*, **34**(5): 698-725.

[10] Perras MA and MS Diederichs 2016. Predicting excavation damage zone depths in brittle rocks. *J. of Rock Mechanics and Geotechnical Engng*, **8**(1): 60-74.

[11] Schofield AN, 1998 (and 2001) The “Mohr-Coulomb” Error. CUED/D-SOILS/TR305; presented in Paris at the scientific jubilee of Pierre Habib; published in “*Mechanique et Geotechnique*”, Balkema 1998.

[12] Wawersik WR and C Fairhurst 1970. A study of brittle rock fracture in laboratory compression experiments. *Int. J. of Rock Mechanics and Mining Sciences*, **7**(5): 561-575.